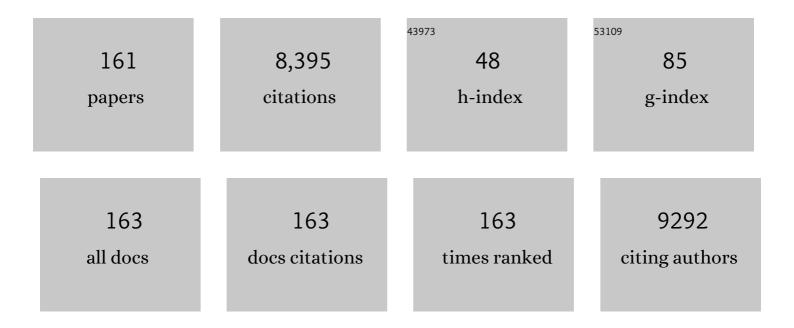
List of Publications by Year in descending order

Source: https://exaly.com/author-pdf/1961687/publications.pdf Version: 2024-02-01



M SATHISH

#	Article	IF	CITATIONS
1	Supercritically exfoliated Bi2Se3 nanosheets for enhanced photocatalytic hydrogen production by topological surface states over TiO2. Journal of Colloid and Interface Science, 2022, 605, 871-880.	5.0	16
2	Dual heteroatoms doped SBA-15 templated porous carbon for symmetric supercapacitor in dual redox additive electrolyte. Journal of Colloid and Interface Science, 2022, 606, 286-297.	5.0	25
3	Surfactant-dependant self organisation of nickel pyrophosphate for electrochemical supercapacitors. Journal of Materials Science: Materials in Electronics, 2022, 33, 9269-9276.	1.1	6
4	lnâ€Situ Synergistic 2D/2D MXene/BCN Heterostructure for Superlative Energy Density Supercapacitor with Superâ€Long Life. Small, 2022, 18, e2106051.	5.2	42
5	Insights into 2D/2D MXene Heterostructures for Improved Synergy in Structure toward Nextâ€Generation Supercapacitors: A Review. Advanced Functional Materials, 2022, 32, .	7.8	152
6	Highly conductive NiSe2 nanoparticle as a co-catalyst over TiO2 for enhanced photocatalytic hydrogen production. Applied Catalysis B: Environmental, 2022, 307, 121159.	10.8	51
7	2D/2D Nanoarchitectured Nb ₂ C/Ti ₃ C ₂ MXene Heterointerface for High-Energy Supercapacitors with Sustainable Life Cycle. ACS Applied Materials & Interfaces, 2022, 14, 21038-21049.	4.0	24
8	Enhanced electrochemical performance of supercritical fluid treated N, P co-doped graphene by dual redox-additives. Journal of Power Sources, 2022, 540, 231587.	4.0	5
9	Titanate quantum dots-sensitized Cu2S nanocomposites for superficial H2 production via photocatalytic water splitting. International Journal of Hydrogen Energy, 2022, 47, 40379-40390.	3.8	11
10	Manifestation of enhanced and durable photocatalytic H2 production using hierarchically structured Pt@Co3O4/TiO2 ternary nanocomposite. Ceramics International, 2021, 47, 10226-10235.	2.3	22
11	CoS2 engulfed ultra-thin S-doped g-C3N4 and its enhanced electrochemical performance in hybrid asymmetric supercapacitor. Journal of Colloid and Interface Science, 2021, 584, 204-215.	5.0	84
12	Enhanced electrochemical performance of supercritical fluid aided P-doped graphene nanoflakes by I3â^'/lâ^' redox couple. Journal of Energy Storage, 2021, 33, 102085.	3.9	5
13	A facile approach to fabricate <i>Saccharum spontaneum</i> -derived porous carbon-based supercapacitors for excellent energy storage performance in redox active electrolytes. Sustainable Energy and Fuels, 2021, 5, 518-531.	2.5	14
14	Solar hydrogen generation from organic substance using earth abundant CuS–NiO heterojunction semiconductor photocatalyst. Ceramics International, 2021, 47, 10206-10215.	2.3	19
15	Design and fabrication of cobalt and nickel ferrites based flexible electrodes for high-performance energy storage applications. Inorganic Chemistry Communication, 2021, 123, 108344.	1.8	22
16	The construction of a dual direct Z-scheme NiAl LDH/g-C ₃ N ₄ /Ag ₃ PO ₄ nanocomposite for enhanced photocatalytic oxygen and hydrogen evolution. Nanoscale Advances, 2021, 3, 2075-2088.	2.2	29
17	Crumpled B, F Co-doped graphene nanosheets for the fabrication of all-solid-state flexible supercapacitors. Chemical Communications, 2021, 57, 8336-8339.	2.2	7
18	Effect of orange peel derived activated carbon as a negative additive for lead-acid battery under high rate discharge condition Journal of Energy Storage, 2021, 34, 102225.	3.9	22

#	Article	IF	CITATIONS
19	Switching the solubility of electroactive ionic liquids for designing high energy supercapacitor and low potential biosensor. Journal of Colloid and Interface Science, 2021, 588, 221-231.	5.0	11
20	Unrevealed Performance of NH ₄ VO ₃ as a Redox-Additive for Augmenting the Energy Density of a Supercapacitor. Journal of Physical Chemistry C, 2021, 125, 8068-8079.	1.5	23
21	Bismuth oxycarbonate Nanoplates@α-Ni(OH)2 nanosheets 2D plate-on-sheet heterostructure as electrode for high-performance supercapacitor. Journal of Alloys and Compounds, 2021, 860, 158495.	2.8	13
22	Redox-Additives in Aqueous, Non-Aqueous, and All-Solid-State Electrolytes for Carbon-Based Supercapacitor: A Mini-Review. Energy & Fuels, 2021, 35, 6465-6482.	2.5	64
23	BiOCl ultrathin nanosheets modified with Fe3+ for enhanced visible light driven photocatalytic activity. Journal of Photochemistry and Photobiology A: Chemistry, 2021, 411, 113211.	2.0	12
24	Black Trumpet Mushroom-like ZnS incorporated with Cu3P: Noble metal free photocatalyst for superior photocatalytic H2 production. Journal of Colloid and Interface Science, 2021, 590, 82-93.	5.0	27
25	One-Pot Hydrothermal Synthesis of Nickel Cobalt Telluride Nanorods for Hybrid Energy Storage Systems. Energy & Fuels, 2021, 35, 12527-12537.	2.5	29
26	Monodispersed core/shell nanospheres of ZnS/NiO with enhanced H2 generation and quantum efficiency at versatile photocatalytic conditions. Journal of Hazardous Materials, 2021, 413, 125359.	6.5	36
27	Fabrication of Flexible Supercapacitor Using N-Doped Porous Activated Carbon Derived from Poultry Waste. Energy & Fuels, 2021, 35, 15094-15100.	2.5	26
28	Gram-scale synthesis of ZnS/NiO core-shell hierarchical nanostructures and their enhanced H2 production in crude glycerol and sulphide wastewater. Environmental Research, 2021, 199, 111323.	3.7	20
29	Metal chalcogenide-based core/shell photocatalysts for solar hydrogen production: Recent advances, properties and technology challenges. Journal of Hazardous Materials, 2021, 415, 125588.	6.5	37
30	Heterojunction engineering at ternary Cu2S/Ta2O5/CdS nanocomposite for enhanced visible light-driven photocatalytic hydrogen evolution. Materials Today Energy, 2021, 21, 100779.	2.5	8
31	Augmenting the electrochemical performance of NiMn2O4 by doping of transition metal ions and compositing with rGO. Journal of Colloid and Interface Science, 2021, 598, 409-418.	5.0	19
32	Surfactant controlled metal oxide shell layer deposition for enhanced photocatalytic solar hydrogen generation: CdSe/TiO2 nanocomposite a case study. Materials Letters, 2021, 298, 130025.	1.3	10
33	MnCo2S4 – MXene: A novel hybrid electrode material for high performance long-life asymmetric supercapattery. Journal of Colloid and Interface Science, 2021, 600, 264-277.	5.0	57
34	TiO2/Carbon allotrope nanohybrids for supercapacitor application with theoretical insights from density functional theory. Applied Surface Science, 2021, 563, 150259.	3.1	14
35	Tailoring the capacitive performance of ZnCo ₂ O ₄ by doping of Ni ²⁺ and fabrication of asymmetric supercapacitor. New Journal of Chemistry, 2021, 45, 21919-21927.	1.4	5
36	Temperature-Driven Morphology Control on CdSe Nanofractals and Its Influence over the Augmented Rate of H ₂ Evolution: Charge Separation via the S-Scheme Mechanism with Incorporated Cu ₃ P. ACS Applied Energy Materials, 2021, 4, 13983-13996.	2.5	17

#	Article	IF	CITATIONS
37	CuO@NiO core-shell nanoparticles decorated anatase TiO2 nanospheres for enhanced photocatalytic hydrogen production. International Journal of Hydrogen Energy, 2020, 45, 7517-7529.	3.8	59
38	Tuning the type of nitrogen on N-RGO supported on N-TiO2 under ultrasonication/hydrothermal treatment for efficient hydrogen evolution – A mechanistic overview. Ultrasonics Sonochemistry, 2020, 64, 104866.	3.8	11
39	Enhancement of photocatalytic H2 evolution from water splitting by construction of two dimensional gC3N4/NiAl layered double hydroxides. Applied Surface Science, 2020, 509, 144656.	3.1	59
40	Electrochemical Performance of Thespesia Populnea Seeds Derived Activated Carbon - Supercapacitor and Its Improved Specific Energy in Redox Additive Electrolytes. Journal of Energy Storage, 2020, 32, 101939.	3.9	30
41	Waste engine oil derived porous carbon/ZnS Nanocomposite as Bi-functional electrocatalyst for supercapacitor and oxygen reduction. Journal of Energy Storage, 2020, 32, 101774.	3.9	15
42	New Method for the Synthesis of 2D Vanadium Nitride (MXene) and Its Application as a Supercapacitor Electrode. ACS Omega, 2020, 5, 17983-17992.	1.6	84
43	High-Performance High-Voltage Symmetric Supercapattery Based on a Graphitic Carbon Nitride/Bismuth Vanadate Nanocomposite. Energy & Fuels, 2020, 34, 16858-16869.	2.5	17
44	Boosting the Energy Density of Flexible Supercapacitors by Redox-Additive Hydrogels. Energy & Fuels, 2020, 34, 11536-11546.	2.5	28
45	Na ₂ MoO ₄ -Incorporated Polymer Gel Electrolyte for High Energy Density Flexible Supercapacitor. ACS Applied Energy Materials, 2020, 3, 11368-11377.	2.5	49
46	Ultrasound-Assisted Room Temperature Synthesis of Flower-Like-Bi ₅ O ₇ I-Incorporated Reduced Graphene Oxide Nanosheets for Highly Efficient Visible-Light Photocatalytic Activity. Journal of Physical Chemistry C, 2020, 124, 20898-20910.	1.5	12
47	Enhancement in the Specific Energy of Bâ€doped Graphene Using Redox Additive Electrolytes. ChemistrySelect, 2020, 5, 9825-9833.	0.7	16
48	Transformation of multilayer WS2 nanosheets to 1D luminescent WS2 nanostructures by one-pot supercritical fluid processing for hydrogen evolution reaction. Materials Science in Semiconductor Processing, 2020, 119, 105167.	1.9	10
49	Synthesis of Ag and N doped potassium tantalate perovskite nanocubes for enhanced photocatalytic hydrogen evolution. Materials Letters, 2020, 275, 128166.	1.3	10
50	Efficient electrocatalytic activity for oxygen reduction reaction by phosphorus-doped graphene using supercritical fluid processing. Bulletin of Materials Science, 2020, 43, 1.	0.8	8
51	The fascinating supercapacitive performance of activated carbon electrodes with enhanced energy density in multifarious electrolytes. Sustainable Energy and Fuels, 2020, 4, 3029-3041.	2.5	60
52	Retorting Photocorrosion and Enhanced Charge Carrier Separation at CdSe Nanocapsules by Chemically Synthesized TiO ₂ Shell for Photocatalytic Hydrogen Fuel Generation. ChemCatChem, 2020, 12, 3139-3152.	1.8	17
53	A simple, economical one-pot microwave assisted synthesis of nitrogen and sulfur co-doped graphene for high energy supercapacitors. Electrochimica Acta, 2020, 341, 135999.	2.6	42
54	Sandwich layered Li0.32Al0.68MnO2(OH)2 from spent Li-ion battery to build high-performance supercapacitor: Waste to energy storage approach. Journal of Alloys and Compounds, 2020, 827, 154336.	2.8	25

#	Article	IF	CITATIONS
55	Fe (III) ions grafted bismuth oxychloride nanosheets for enhanced electrochemical supercapacitor application. Journal of Electroanalytical Chemistry, 2020, 862, 113958.	1.9	14
56	Investigations on the nature of electrolyte on the electrochemical supercapacitor performance of heteroatom doped graphene. Ionics, 2020, 26, 2081-2094.	1.2	10
57	Effective coupling of Cu (II) with BiOCl nanosheets for high performance electrochemical supercapacitor and enhanced photocatalytic applications. Applied Surface Science, 2020, 521, 146362.	3.1	39
58	Hydrothermal synthesis of cobalt telluride nanorods for a high performance hybrid asymmetric supercapacitor. RSC Advances, 2020, 10, 13632-13641.	1.7	53
59	High and reversible oxygen uptake in carbon dot solutions generated from polyethylene facilitating reactant-enhanced solar light harvesting. Nanoscale, 2020, 12, 10480-10490.	2.8	15
60	Investigation of electrochemical supercapacitor performance of WO3-CdS nanocomposites in 1ÂM H2SO4 electrolyte prepared by microwave-assisted method. Materials Letters, 2020, 274, 127998.	1.3	18
61	Heterojunction of CdS Nanocapsules–WO ₃ Nanosheets Composite as a Stable and Efficient Photocatalyst for Hydrogen Evolution. Energy & Fuels, 2020, 34, 14598-14610.	2.5	22
62	Construction of heterostructure based on hierarchical Bi ₂ MoO ₆ and g-C ₃ N ₄ with ease for impressive performance in photoelectrocatalytic water splitting and supercapacitor. Catalysis Science and Technology, 2020, 10, 2427-2442.	2.1	43
63	Supercritical water assisted preparation of recyclable gold nanoparticles and their catalytic utility in cross-coupling reactions under sustainable conditions. Nanoscale Advances, 2019, 1, 3177-3191.	2.2	18
64	Sustainable hydrogen production for the greener environment by quantum dots-based efficient photocatalysts: A review. Journal of Environmental Management, 2019, 248, 109246.	3.8	122
65	Supercritical fluid assisted synthesis of S-doped graphene and its symmetric supercapacitor performance evaluation using different electrolytes. Synthetic Metals, 2019, 255, 116111.	2.1	26
66	Transformation of sluggish higher valent molybdenum into electrocatalytically active amorphous carbon doped MoO2/MoO3-x nanostructures using phyllanthus reticulatus fruit extract as natural reducing agent in supercritical fluid processing. International Journal of Hydrogen Energy, 2019, 44, 21692-21702.	3.8	7
67	Waste Toner-Derived Carbon/Fe ₃ O ₄ Nanocomposite for High-Performance Supercapacitor. ACS Omega, 2019, 4, 15798-15805.	1.6	56
68	Fabrication of 9.6 V High-performance Asymmetric Supercapacitors Stack Based on Nickel Hexacyanoferrate-derived Ni(OH)2 Nanosheets and Bio-derived Activated Carbon. Scientific Reports, 2019, 9, 1104.	1.6	105
69	Synthesis of Boronâ€Doped Graphene by Supercritical Fluid Processing and its Application in Symmetric Supercapacitors using Various Electrolytes. ChemElectroChem, 2019, 6, 1492-1499.	1.7	40
70	Performance evaluation of B-doped graphene prepared via two different methods in symmetric supercapacitor using various electrolytes. Applied Surface Science, 2019, 491, 560-569.	3.1	50
71	Ultrasonically aided selective stabilization of pyrrolic type nitrogen by one pot nitrogen doped and hydrothermally reduced Graphene oxide/Titania nanocomposite (N-TiO2/N-RGO) for H2 production. Ultrasonics Sonochemistry, 2019, 57, 62-72.	3.8	23
72	Photocatalytic recovery of H2 from H2S containing wastewater: Surface and interface control of photo-excitons in Cu2S@TiO2 core-shell nanostructures. Applied Catalysis B: Environmental, 2019, 254, 174-185.	10.8	209

#	Article	IF	CITATIONS
73	Electrochemical investigation of hybridized WO3–CdS semiconducting nanostructures prepared by microwave-assisted wet chemical route for supercapacitor application. Journal of Materials Science: Materials in Electronics, 2019, 30, 9231-9244.	1.1	6
74	Synthesis of GNS-MnS hybrid nanocomposite for enhanced electrochemical energy storage applications. Materials Chemistry and Physics, 2019, 230, 249-257.	2.0	22
75	Preparation and comparison of hybridized WO3–V2O5 nanocomposites electrochemical supercapacitor performance in KOH and H2SO4 electrolyte. Materials Letters, 2019, 236, 702-705.	1.3	22
76	Investigating the synergistic effect of hybridized WO3-ZnS nanocomposite prepared by microwave-assisted wet chemical method for supercapacitor application. Journal of Electroanalytical Chemistry, 2019, 833, 93-104.	1.9	21
77	Facile synthesis of ZnO nanoflowers/reduced graphene oxide nanocomposite using zinc hexacyanoferrate for supercapacitor applications. Materials Letters, 2019, 236, 424-427.	1.3	45
78	Cauliflower-like CuS/ZnS nanocomposites decorated g-C3N4 nanosheets as noble metal-free photocatalyst for superior photocatalytic water splitting. Chemical Engineering Journal, 2019, 360, 1277-1286.	6.6	119
79	Longâ€termâ€durable antiâ€icing superhydrophobic composite coatings. Journal of Applied Polymer Science, 2019, 136, 47059.	1.3	22
80	Dwindling the re-stacking by simultaneous exfoliation of boron nitride and decoration of α-Fe ₂ O ₃ nanoparticles using a solvothermal route. New Journal of Chemistry, 2018, 42, 5090-5095.	1.4	8
81	Nanostructured semiconducting materials for efficient hydrogen generation. Environmental Chemistry Letters, 2018, 16, 765-796.	8.3	97
82	One-dimensional growth of hexagonal rods of metastable h-MoO3 using one-pot, rapid and environmentally benign supercritical fluid processing. Physica E: Low-Dimensional Systems and Nanostructures, 2018, 99, 189-193.	1.3	14
83	Effective shuttling of photoexcitons on CdS/NiO core/shell photocatalysts for enhanced photocatalytic hydrogen production. Materials Research Bulletin, 2018, 101, 223-231.	2.7	53
84	Fabrication of robust superhydrophobic coatings using <scp>PTFEâ€MWCNT</scp> nanocomposite: Supercritical fluid processing. Surface and Interface Analysis, 2018, 50, 464-470.	0.8	13
85	Structural and electrochemical studies of tungsten oxide (WO3) nanostructures prepared by microwave assisted wet-chemical technique for supercapacitor. Journal of Materials Science: Materials in Electronics, 2018, 29, 6157-6166.	1.1	22
86	Synthesis of titania wrapped cadmium sulfide nanorods for photocatalytic hydrogen generation. Materials Research Bulletin, 2018, 103, 122-132.	2.7	43
87	CuO Cr 2 O 3 core-shell structured co-catalysts on TiO 2 for efficient photocatalytic water splitting using direct solar light. International Journal of Hydrogen Energy, 2018, 43, 3976-3987.	3.8	40
88	Supercritical fluid processing of N-doped graphene and its application in high energy symmetric supercapacitor. International Journal of Hydrogen Energy, 2018, 43, 4044-4057.	3.8	48
89	Electrochemical investigation of manganese ferrites prepared via a facile synthesis route for supercapacitor applications. Colloids and Surfaces A: Physicochemical and Engineering Aspects, 2018, 538, 668-677.	2.3	76
90	Development of high quantum efficiency CdS/ZnS core/shell structured photocatalyst for the enhanced solar hydrogen evolution. International Journal of Hydrogen Energy, 2018, 43, 22315-22328.	3.8	42

#	Article	IF	CITATIONS
91	Symmetric electrochemical supercapacitor performance evaluation of N-doped graphene prepared via supercritical fluid processing. Journal of Solid State Electrochemistry, 2018, 22, 3821-3832.	1.2	16
92	Investigation of electrochemical properties of microwave irradiated tungsten oxide (WO ₃) nanorod structures for supercapacitor electrode in KOH electrolyte. Materials Research Express, 2018, 5, 085007.	0.8	16
93	NiTe Nanorods as Electrode Material for High Performance Supercapacitor Applications. ChemistrySelect, 2018, 3, 9034-9040.	0.7	41
94	Electrochemical cycling and beyond: unrevealed activation of MoO ₃ for electrochemical hydrogen evolution reactions. Chemical Communications, 2017, 53, 2245-2248.	2.2	38
95	All-solid-state asymmetric supercapacitors based on cobalt hexacyanoferrate-derived CoS and activated carbon. RSC Advances, 2017, 7, 6648-6659.	1.7	184
96	Electrochemical Studies on Corncob Derived Activated Porous Carbon for Supercapacitors Application in Aqueous and Non-aqueous Electrolytes. Electrochimica Acta, 2017, 228, 586-596.	2.6	171
97	Anchoring of ultrafine Co ₃ O ₄ nanoparticles on MWCNTs using supercritical fluid processing and its performance evaluation towards electrocatalytic oxygen reduction reaction. Catalysis Science and Technology, 2017, 7, 1227-1234.	2.1	29
98	Shape dependence structural, optical and photocatalytic properties of TiO2 nanocrystals for enhanced hydrogen production via glycerol reforming. Solar Energy Materials and Solar Cells, 2017, 163, 113-119.	3.0	60
99	Mechanical activation on aluminothermic reduction and magnetic properties of NiO powders. Journal Physics D: Applied Physics, 2017, 50, 21LT01.	1.3	10
100	Multifunctional Cu/Ag quantum dots on TiO 2 nanotubes as highly efficient photocatalysts for enhanced solar hydrogen evolution. Journal of Catalysis, 2017, 350, 226-239.	3.1	103
101	Mitigating the Surface Degradation and Voltage Decay of Li _{1.2} Ni _{0.13} Mn _{0.54} Co _{0.13} O ₂ Cathode Material through Surface Modification Using Li ₂ ZrO ₃ . ACS Omega, 2017, 2, 2308-2316.	1.6	41
102	Enhanced Superhydrophobic Performance of BN-MoS ₂ Heterostructure Prepared via a Rapid, One-Pot Supercritical Fluid Processing. Langmuir, 2017, 33, 6159-6166.	1.6	21
103	High-performance Solid-state Hybrid Energy-storage Device Consisting of Reduced Graphene-Oxide Anchored with NiMn-Layered Double Hydroxide. Electrochimica Acta, 2017, 236, 359-370.	2.6	53
104	Soya derived heteroatom doped carbon as a promising platform for oxygen reduction, supercapacitor and CO2 capture. Carbon, 2017, 114, 679-689.	5.4	134
105	Biomass-Derived Activated Porous Carbon from Rice Straw for a High-Energy Symmetric Supercapacitor in Aqueous and Non-aqueous Electrolytes. Energy & Fuels, 2017, 31, 977-985.	2.5	291
106	Supercritical fluid processing for the synthesis of NiS ₂ nanostructures as efficient electrocatalysts for electrochemical oxygen evolution reactions. Catalysis Science and Technology, 2017, 7, 3591-3597.	2.1	44
107	Supercriticalâ€Fluidâ€Assisted Decoration of MoS ₂ @ MWCNTs and Their Superior Performance in the Electrochemical Hydrogen Evolution Reaction. ChemistrySelect, 2017, 2, 5978-5983.	0.7	5
108	Orange Peel Derived Activated Carbon for Fabrication of Highâ€Energy and Highâ€Rate Supercapacitors. ChemistrySelect, 2017, 2, 11384-11392.	0.7	103

#	Article	IF	CITATIONS
109	Grapheneâ€Polymer//Grapheneâ€Manganese Oxide Nanocompositesâ€Based Asymmetric High Energy Supercapacitor with 1.8â€V Cell Voltage in Aqueous Solution. ChemistrySelect, 2017, 2, 10754-10761.	0.7	17
110	Template Assisted Synthesis of Nitrogen doped 3D-Graphene for Supercapacitor Applications. Materials Today: Proceedings, 2017, 4, 12144-12151.	0.9	5
111	Synthesis of Novel La 0.7 Ce 0.2 Sr 0.1 Fe 0.5 Mn 0.4 Co 0.1 O 3 (LCSFMCO) Perovskite Nanoparticles and Characterization for Structural, Electrochemical Properties. Materials Today: Proceedings, 2017, 4, 12198-12204.	0.9	2
112	N-Containing Carbon/Graphene Nanocomposites for Electrochemical Supercapacitor Applications. Journal of Nanoscience and Nanotechnology, 2017, 17, 1267-1274.	0.9	2
113	Supercritical Fluid Facilitated Disintegration of Hexagonal Boron Nitride Nanosheets to Quantum Dots and Its Application in Cells Imaging. ACS Applied Materials & Interfaces, 2016, 8, 18647-18651.	4.0	56
114	High performance supercapacitor using N-doped graphene prepared via supercritical fluid processing with an oxime nitrogen source. Electrochimica Acta, 2016, 200, 37-45.	2.6	71
115	Facile and Scalable Ultra–fine Cobalt Oxide/Reduced Graphene Oxide Nanocomposites for High Energy Asymmetric Supercapacitorsâ€. ChemistrySelect, 2016, 1, 3455-3467.	0.7	58
116	Selective growth of fullerene octahedra and flower-like particles by a liquid–liquid interfacial precipitation method for super-hydrophobic applications. RSC Advances, 2016, 6, 78791-78794.	1.7	11
117	<i>Aloe vera</i> Derived Activated High-Surface-Area Carbon for Flexible and High-Energy Supercapacitors. ACS Applied Materials & amp; Interfaces, 2016, 8, 35191-35202.	4.0	198
118	Facile and scalable route to sheets-on-sheet mesoporous Ni–Co-hydroxide/reduced graphene oxide nanocomposites and their electrochemical and magnetic properties. RSC Advances, 2016, 6, 15941-15951.	1.7	29
119	Synthesis of nanostructured Cu-WO3 and CuWO4 for supercapacitor applications. Journal of Materials Science: Materials in Electronics, 2016, 27, 2926-2932.	1.1	33
120	Rapid, one-pot synthesis of luminescent MoS ₂ nanoscrolls using supercritical fluid processing. Journal of Materials Chemistry C, 2016, 4, 1165-1169.	2.7	46
121	Vortex-Aligned Fullerene Nanowhiskers as a Scaffold for Orienting Cell Growth. ACS Applied Materials & Interfaces, 2015, 7, 15667-15673.	4.0	112
122	Supercritical fluid processing: a rapid, one-pot exfoliation process for the production of surfactant-free hexagonal boron nitride nanosheets. CrystEngComm, 2015, 17, 5895-5899.	1.3	75
123	A 2ÂV asymmetric supercapacitor based on reduced graphene oxide-carbon nanofiber-manganese carbonate nanocomposite and reduced graphene oxide in aqueous solution. Journal of Solid State Electrochemistry, 2015, 19, 2311-2320.	1.2	24
124	Electrochemical Characterization of Catalytic Activities of C60Nanowhiskers to Oxygen Reduction in Aqueous Solution. Fullerenes Nanotubes and Carbon Nanostructures, 2015, 23, 509-512.	1.0	10
125	Manganese hexacyanoferrate derived Mn3O4 nanocubes–reduced graphene oxide nanocomposites and their charge storage characteristics in supercapacitors. Physical Chemistry Chemical Physics, 2014, 16, 4952.	1.3	120
126	Supercritical fluid assisted synthesis of N-doped graphene nanosheets and their capacitance behavior in ionic liquid and aqueous electrolytes. Journal of Materials Chemistry A, 2014, 2, 4731-4738.	5.2	72

#	Article	IF	CITATIONS
127	Functionalization of graphene with nitrogen using ethylenediaminetetraacetic acid and their electrochemical energy storage properties. RSC Advances, 2014, 4, 24248.	1.7	20
128	Supercritical fluid processing of nitric acid treated nitrogen doped graphene with enhanced electrochemical supercapacitance. RSC Advances, 2014, 4, 52256-52262.	1.7	52
129	Graphene and Graphene-Based Nanocomposites for Electrochemical Energy Storage. , 2014, , 221-248.		0
130	Alcohol-induced decomposition of Olmstead's crystalline Ag(<scp>i</scp>)–fullerene heteronanostructure yields â€~bucky cubes'. Journal of Materials Chemistry C, 2013, 1, 1174-1181.	2.7	61
131	Superhydrophilic Graphene-Loaded TiO ₂ Thin Film for Self-Cleaning Applications. ACS Applied Materials & Interfaces, 2013, 5, 207-212.	4.0	210
132	Synthesis and Electrochemical Properties of Biporous <l>α</l> -Fe ₂ O ₃ Superstructures. Journal of Nanoscience and Nanotechnology, 2013, 13, 6635-6643.	0.9	1
133	Advanced Energy Devices: Lithium Ion Battery and High Energy Capacitor. , 2013, , 1149-1173.		2
134	Graphene anchored with Fe3O4 nanoparticles as anode for enhanced Li-ion storage. Journal of Power Sources, 2012, 217, 85-91.	4.0	104
135	Ultrathin SnS ₂ Nanoparticles on Graphene Nanosheets: Synthesis, Characterization, and Li-Ion Storage Applications. Journal of Physical Chemistry C, 2012, 116, 12475-12481.	1.5	137
136	Synthesis and Characterization of Fullerene Nanowhiskers by Liquid-Liquid Interfacial Precipitation: Influence of C60 Solubility. Molecules, 2012, 17, 3858-3865.	1.7	43
137	Nanocrystalline tin compounds/graphene nanocomposite electrodes as anode for lithium-ion battery. Journal of Solid State Electrochemistry, 2012, 16, 1767-1774.	1.2	30
138	Nanographene derived from carbon nanofiber and its application to electric double-layer capacitors. Electrochimica Acta, 2012, 68, 146-152.	2.6	24
139	Crystallization-Induced Top-Down Wormlike Hierarchical Porous α-Fe2O3 Self-Assembly. Journal of Physical Chemistry C, 2011, 115, 6367-6374.	1.5	17
140	Facile Fabrication of Hierarchical α-Fe ₂ O ₃ : Self-Assembly and Its Magnetic and Electrochemical Properties. Journal of Physical Chemistry C, 2011, 115, 18164-18173.	1.5	38
141	MnO2 assisted oxidative polymerization of aniline on graphene sheets: Superior nanocomposite electrodes for electrochemical supercapacitors. Journal of Materials Chemistry, 2011, 21, 16216.	6.7	63
142	Fullerene nanowhiskers at liquid–liquid interface: A facile template for metal oxide (TiO2, CeO2) nanofibers and their photocatalytic activity. Materials Chemistry and Physics, 2011, 130, 211-217.	2.0	11
143	Open-Mouthed Metallic Microcapsules: Exploring Performance Improvements at Agglomeration-Free Interiors. Journal of the American Chemical Society, 2010, 132, 14415-14417.	6.6	89
144	Selective precipitation of tubular-like short fullerene (C60) whiskers at liquid–liquid interface. CrystEngComm, 2010, 12, 4146.	1.3	17

#	ARTICLE	IF	CITATIONS
145	N,S-Co-doped TiO ₂ Nanophotocatalyst: Synthesis, Electronic Structure and Photocatalysis. Journal of Nanoscience and Nanotechnology, 2009, 9, 423-432.	0.9	65
146	Solvent Engineering for Shape-Shifter <i>Pure</i> Fullerene (C ₆₀). Journal of the American Chemical Society, 2009, 131, 6372-6373.	6.6	183
147	Preparation and Optical Properties of Fullerene/Ferrocene Hybrid Hexagonal Nanosheets and Large-Scale Production of Fullerene Hexagonal Nanosheets. Journal of the American Chemical Society, 2009, 131, 9940-9944.	6.6	107
148	Preparation, characterization, and electrochemical application of metal/metal ion loaded fullerene nanowhiskers. Journal of Solid State Electrochemistry, 2008, 12, 835-840.	1.2	13
149	Preparation and characterization of Ni incorporated fullerene nanowhiskers. Diamond and Related Materials, 2008, 17, 571-575.	1.8	20
150	ORGANIC-METAL-DOPED FULLERENE NANOWHISKERS. Nano, 2008, 03, 351-354.	0.5	6
151	Fe -DECORATED FULLERENE (C ₆₀) NANOWHISKERS FOR ENVIRONMENTAL APPLICATION. Nano, 2008, 03, 409-414.	0.5	8
152	INFLUENCE OF HETEROATOM DOPING OF TIO2 NANOPARTICLE ON THE RED SHIFT AND THE RELATED CATALYTIC ACTIVITY. International Journal of Nanoscience, 2007, 06, 137-141.	0.4	3
153	Ultrasonic-mediated Preparation of Mesoporous Crystalline CdS Nanoparticle. Chemistry Letters, 2007, 36, 948-949.	0.7	2
154	Photocatalytic generation of hydrogen over mesoporous CdS nanoparticle: Effect of particle size, noble metal and support. Catalysis Today, 2007, 129, 421-427.	2.2	98
155	Characterization and photocatalytic activity of N-doped TiO2 prepared by thermal decomposition of Ti–melamine complex. Applied Catalysis B: Environmental, 2007, 74, 307-312.	10.8	123
156	Nanoporous Fullerene Nanowhiskers. Chemistry of Materials, 2007, 19, 2398-2400.	3.2	100
157	Size-Tunable Hexagonal Fullerene (C ₆₀) Nanosheets at the Liquidâ^'Liquid Interface. Journal of the American Chemical Society, 2007, 129, 13816-13817.	6.6	179
158	Alternate synthetic strategy for the preparation of CdS nanoparticles and its exploitation for water splitting. International Journal of Hydrogen Energy, 2006, 31, 891-898.	3.8	267
159	W17I SYNTHESIS AND CHARACTERIZATION OF FULLERENE NANOWHISKERS USING LIQUID-LIQUID INTERFACIAL PRECIPITATION(International Workshop on "New Frontiers of Smart Materials and Structural) Tj ETQq1 1 0.7843		Ov e rlock 10
160	Synthesis, Characterization, Electronic Structure, and Photocatalytic Activity of Nitrogen-Doped TiO2 Nanocatalyst. Chemistry of Materials, 2005, 17, 6349-6353.	3.2	866
161	Electrochemical degradation of aqueous phenols using graphite electrode in a divided electrolytic cell. Korean Journal of Chemical Engineering, 2005, 22, 358-363.	1.2	12